Thin Solid Films 615 (2016) 409–414

Contents lists available at ScienceDirect

Thin Solid Films

journal homepage: www.elsevier.com/locate/tsf

Structural and electronic properties of thermally evaporated V_2O_5 epitaxial thin films

B. Lamoureux [a,*], V.R. Singh [a], V. Jovic [b,c], J. Kuyyalil [a], T.-Y. Su [a], K.E. Smith [a,b,c]

[a] Department of Physics, Boston University, Boston, MA 02215, USA
[b] The MacDiarmid Institute for Advanced Materials and Nanotechnology, New Zealand
[c] School of Chemical Sciences, The University of Auckland, Auckland 92019, New Zealand

ARTICLE INFO

Article history:
Received 17 December 2015
Received in revised form 26 July 2016
Accepted 26 July 2016
Available online 27 July 2016

Keywords:
Vanadium oxide
Thin films
Thermal evaporation
X-ray emission
X-ray absorption

ABSTRACT

This study investigated the physicochemical properties of a V_2O_5 thin film deposited on *c*-plane sapphire through thermal evaporation at a relatively high pressure. Using atomic force microscopy (AFM), X-ray diffraction (XRD) and a suite of X-ray spectroscopic techniques, it was shown that a high quality epitaxial V_2O_5 thin film was achieved. AFM step height analysis demonstrated that the film thickness was ~50 nm with a surface roughness of 1.5 Å, as determined by root mean square roughness measurements. XRD analysis verified that the film was highly crystalline with a (0001) orientation on the substrate. Vanadium was predominantly in the 5+ oxidation state, with contributions from V^{4+} states at the surface, shown by X-ray photoemission spectroscopy analysis X-ray absorption spectroscopy further confirmed the predominant presence of V^{5+} in an octahedral crystal field. The existence with bulk V^{4+} states was shown through V *L*-edge X-ray emission spectroscopy which demonstrated the presence of *d*-*d* crystal field transitions in an otherwise d^0 transition metal oxide. The data suggests that by increasing the partial pressure of oxygen in the vacuum chamber during growth, thermal evaporation can be used as a cheap and efficient way of growing stoichiometric V_2O_5 thin films.

1. Introduction

Correlated oxides, such as vanadium pentoxide (V_2O_5), exhibit diverse electronic and magnetic properties, which can be tuned by varying the carrier density, magnetic field, or strain. This makes these materials promising platforms for the development of nanoscale, multifunctional electronic and spintronic devices [1,2]. Many of the envisioned devices take advantage of the unique electronic properties and easily accessible insulator to semiconductor transition (SIT) as shown in highly stable V_2O_5 thin films (with a SIT of ~257 °C) [3]. For instance, fast electronic switches, coatings on smart windows, and optical shutters have all exploited the ultra-fast SIT as a switching mechanism [4,5]. While these applications are based off the SIT, other devices, like electrochromic displays, utilize the multicolored electro-chromism of crystalline V_2O_5 thin films [1,2]. In the arena of green energy, V_2O_5 has gained attention as a potential means of increasing the energy density of capacitors to improve the storage of electricity [6]. To facilitate the rational design and optimize the performance of such devices, it is important to understand the intrinsic electronic characteristics of V_2O_5. Various methods have been used to grow V_2O_5 thin films, including flash-evaporation of V_2O_5, pulsed-laser deposition, magnetron sputtering, chemical vapor deposition, and spray pyrolysis [7–9]. However, in many of these cases, sub-stoichiometric films (i.e., containing V^{4+}) were obtained [10–14]. These studies also investigated the structural and bulk electronic properties for pure and doped vanadium oxide thin films demonstrating a variety of thicknesses. Not only was a mix of oxidation states obtained, but most films synthesized from these techniques were amorphous or polycrystalline [15]. More generally, a full electronic and structural characterization of highly ordered and smooth V_2O_5 films synthesized by a simple growth technique suitable for advanced synchrotron facilities studies has yet to be reported.

In this study, we describe the fabrication and characterization of an epitaxial V_2O_5 thin film grown on *c*-plane sapphire by a thermal evaporation process at relatively high pressure (~10^{-5} Pa). Thermal evaporation, where a plume of source material is deposited onto a substrate, is found to be a relatively simple and cheap method for growing V_2O_5 films in a well-controlled manner. The morphology of the as-grown films were examined using X-ray diffraction (XRD), atomic forced microscopy (AFM) and X-ray photoemission spectroscopy (XPS). In addition, we apply XPS along with X-ray absorption (XAS) and X-ray emission spectroscopy (XES) to investigate the surface and bulk electronic properties of the as-grown V_2O_5 thin film [16–18].

2. Experimental

V_2O_5 powder (>99.6%) was deposited from a tantalum boat onto *c*-plane (0001) sapphire via thermal evaporation. The film was grown in a high vacuum chamber with a base pressure of 10^{-5} Pa. Prior to growth, the substrate surface was cleaned by firstly rinsing with deionized water, then dipping in 1:1:100 H_2O_2:NaOH:H_2O, and finally

http://dx.doi.org/10.1016/j.tsf.2016.07.062
0040-6090/

sonicating the substrate in ethanol. Growth was achieved by passing 35 A of current through a tungsten filament (wrapped around the tantalum boat) for half an hour. No post deposition annealing was performed following growth.

Crystal phase analysis of the V_2O_5 thin film was carried out using a Bruker D8 high resolution XRD. Radiation from a Cu K_α source ($\lambda = 1.5418$ Å) was refined by a Gobel mirror to filter Cu K_β radiation, and two 0.2 mm width slits; one positioned directly in front of the sample and the other directly prior to the lynxeye detector. The system was operated at 45 kV and 40 mA with an angular resolution of 0.001° across a 2θ range of 15–65°. The surface morphology and thickness of the thin film was also examined using a Digital Instruments AFM in the tapping mode.

XPS data were collected using a hemispherical analyzer with monochromatic X-rays generated by an aluminum K_α anode. The base pressure of the vacuum chamber was 2.4×10^{-7} Pa during measurements. The spectra were calibrated against the C 1*s* signal from adventitious hydrocarbons. XAS and XES were both performed at beamline 8.0.1 of the Advanced Light Source, Berkeley, CA. XAS measurements were performed in both the more surface sensitive total electron yield (TEY) mode, with a penetration depth of ~10 nm, and in the more bulk sensitive total fluorescence yield (TFY) mode, with a probing depth of ~100 nm. Agreement between TEY and TFY spectra indicated that the sample did not charge during measurements, and that the TEY signal was also illustrative of the bulk. The energy scales of XAS spectra at the V *L*- and O *K*-edges were calibrated with reference to the Ti *L*- and O *K*-edge XAS spectra of rutile TiO_2. Spectral resolution was ~200 meV at full width at half maximum (FWHM). The photon flux was 2.2×10^{12} photon s^{-1}. XES spectral resolution was 700 meV. XES data were calibrated with reference to the $L\alpha_{1,2}$ and $L_{\beta1}$ second order emission lines of Zn. The analysis chamber pressure was below 10^{-7} Pa during XAS and XES measurements.

To remove undesirable high frequency noise components from the intensity signals of noisy spectra, a Finite Impulse Response (FIR) Low Pass (LP) filtering method was implemented. The method has been described comprehensively in our previous publications [19,20].

3. Results and discussion

The XRD pattern, presented in Fig. 1(a), shows a singly oriented, or epitaxial, V_2O_5 thin film deposited onto *c*-plane sapphire via thermal evaporation. A sapphire substrate was chosen as both α-Al_2O_3 and V_2O_5 are in the same space group (R3*c*), thus the lattice parameters will be well matched to the natural bond lengths of V_2O_5 [21]. As determined by XRD, the film is oriented in the (110) direction, with a lattice constant of 4.95 Å. The FWHM of the (220) reflection was found to be 0.11°, suggesting that the film is highly crystalline. AFM images (displayed in Fig. 1(b)) show smooth surfaces with root mean square roughness of ~1.5 Å. The relatively smooth film surface reflects the effectiveness of the substrate cleaning procedure described within in the experimental section. AFM depth profiling indicated that the thickness is approximately 50 nm (Fig. 1c). Films grown under comparable conditions by atomic layer deposition, which is considered a more

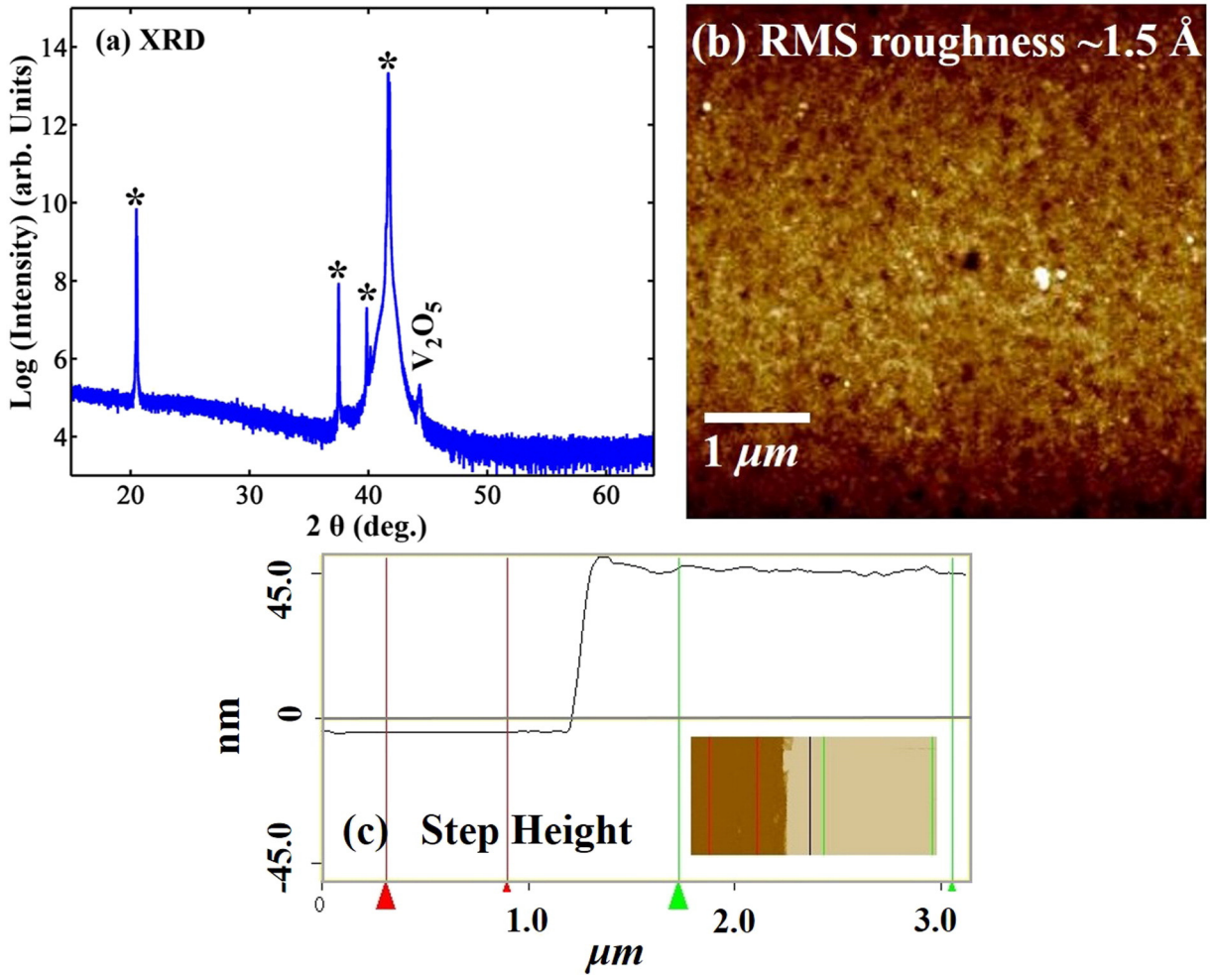

Fig. 1. (a) XRD θ–2θ scans for a 50 nm V_2O_5 film grown on a *c*-sapphire substrate. (b) AFM images of the 50 nm V_2O_5 film showing a clear, flat and smooth surface, with a root mean square roughness of 1.5 Å. (c) Step heights through AFM shows that the film thickness is ~50 nm.

refined technique than thermal evaporation, exhibited an equivalent surface roughness at a similar thickness [22].

Fig. 2 shows an XPS survey scan of the V_2O_5 thin film across a binding energy range of 0–1250 eV. A V 2*p* core level XPS scan is shown at the inset. In addition, the binding energies (E_B) and FWHM values of critical core levels are listed in Table 1. As indicated on the survey scan, the identified peaks correspond to photoelectron emission from carbon, vanadium, and oxygen. This would suggest that the film was atomically clean apart from the expected presence of adventitious hydrocarbons. Fig. 3(a) and (b) shows V $2p_{3/2}$ and O 1*s* core level scans, respectively, for the V_2O_5 thin film. Both the V $2p_{3/2}$ and O 1*s* core level features were fitted with two peaks, corresponding to contributions from V^{5+} and V^{4+} oxidation states, as denoted by subscripts A and B, respectively in Fig. 3. The fitted peaks at E_B(V $2p_{3/2A}$) = 516.98 eV, E_B(V $2p_{3/2B}$) = 515.5 eV, E_B (O $1s_A$) = 530.00 eV, and E_B(O $1s_B$) = 530.80 eV (summarized in Table 1) are in excellent agreement with previous experiments and indicate that vanadium is predominantly exists in the 5 + oxidation state [23,24]. Because XPS is a surface sensitive measurement, by taking the ratio of the area between the V^{5+} fitted peak and the total peak area it was found that 75% of the surface layer exists in the V^{5+} oxidation state. It should be noted that the same calculation used to obtain the percentages of V^{5+} and V^{4+} at the surface could be performed using the O 1*s* peak. However, as the difference in energy between O $1s_A$ and O $1s_B$ is almost half that of the corresponding value for the V $2p_{3/2A}$ and V $2p_{3/2B}$, computing the ratio of oxidation states present by this method is less reliable.

The stoichiometry of the film was calculated from the peak areas at E_B (V $2p_{3/2A}$) = 516.98 eV and E_B (O $1s_A$) = 530.0 eV using;

$$\frac{N_i}{N_j} = \frac{I_i}{I_i}\frac{\lambda_j \sigma_j T_j}{\lambda_i \sigma_j T_j} \quad (1)$$

here, N_i is the number of moles, I_i the background corrected intensities or peak areas of the photoelectron emission line, λ_i the attenuation length, σ_i the atomic sensitivity factor for photoionization, and T_i is the transmission coefficient of the spectrometer for the photoelectrons emitted by oxygen, denoted by subscript *i*, and V, denoted by subscript *j*. The O:V ratio is equal to 2.55. The stoichiometric ratio calculated from this method is within 2% error of V_2O_5. A high degree of crystallinity present in the film is shown by the largest FWHM of a V_2O_5 peak being small (2.94 eV) [23–26]. These observations are consistent with the XRD results presented in Fig. 1a.

XAS, a powerful method of addressing the electronic structure of complex materials, was used to probe the unoccupied element-specific partial density of states (pDOS). Fig. 4(a) shows V *L*-edge XAS spectra in both the TEY (black) and TFY (red) modes. The V *L*-edge spectra are dominated by two regions; L_3 (transitions from V $2p_{3/2}$ core levels into unoccupied V 3*d* states) and L_2 (transitions from V $2p_{1/2}$ core levels into unoccupied V 3*d* states). The main feature on the L_2 (~525.8 eV) has been attributed to the e_g molecular orbital [16]. Crystal field splitting within the V 3*d* states splits the L_3 edge into the t_{2g} (~516.6 eV and ~517.8 eV) and e_g (~519.5 eV) molecular orbital levels due to the approximate octahedral geometry. Spectral broadening observed in the TEY mode as compared to the equivalent TFY spectra is attributed to surface contamination, which is also supported through the appearance of C 1*s* peak in the XPS spectra (Fig. 2d). While electronic features from both oxidation states were readily seen in the XPS spectra, the characteristic doublet of V^{4+} is masked by the much larger V^{5+} signal. Contributions from V^{3+} states are not evident in any of the spectra. Based on the observations of Mendialdua et al. [25], the peak energies in the V 2*p* spectrum are consistent with the V^{5+} oxidation state (Fig. 3a). Due to the consistency in the overall spectral shape between the TEY and TFY data, the film is believed to be homogeneous.

Fig. 4(b) shows O *K*-edge XAS spectra for V_2O_5 in the TEY (black) and TFY (red) modes. X-ray absorption at the O *K*-edge corresponds to transitions from O 1*s* core levels to unoccupied O 2*p* states within the CB. The large absorption intensity provides a good indication of covalent interactions within the material. From the parent molecular orbitals, the primary metal character of each band can be inferred [22–35]. A prominent doublet near the onset of absorption, ~528–535 eV, is attributed to O 2*p* states hybridized with V 3*d* states in an octahedral crystal field. This splitting of the O *K*-edge is the result of both ionic and covalent contributions. Briefly, in V_2O_5 the V $3d_z^2$ and V $3d_{x^2-y}^2$ states have the greatest overlap with the oxygen ligand states, resulting in the formation of σ bonding and σ* anti-bonding molecular orbitals upon interaction with the O 2*p* states. Similarly, the V $3d_{xz}$ and V $3d_{yz}$ linearly combine with the O 2*p* orbitals, forming π bonding and π* antibonding molecular orbitals. Thus, the σ* is the highest energy antibonding orbital as it is comprised of atomic orbitals which have the most overlap. The energy of the σ* and π* molecular orbitals was found to be 532.51 eV and 530.24 eV, respectively. The O *K*-edge splitting observed in Fig. 4b, which is a direct consequence of the formation of σ*, is a general feature of vanadium oxides, however the distribution of intensity within the O *K*-edge is unique to the geometric structure. Unsurprisingly, XAS on single crystal phase V_2O_5 reflects the same splitting pattern, which further supports this molecular description for orbital splitting [36].

The intensity of the different features at the O *K*-edge absorption edge is related to the strength of the metal-ligand hybridization. This is directly reflected in the relative intensity of the hybridized O 2*p*-V 3*d* bands, which increase with respect to the V 4*sp* bands as one goes from V_2O_3 to V_2O_5 [28]. Fig. 4(a) and (b) shows that there is a marked increase in the relative intensity of V 3*d* bands with respect to the V 4*sp* bands between VO_2 and V_2O_5. This enhancement is related to increased V 3*d* to O 2*p* hybridization for higher vanadium valences, in turn indicating that the contribution of the V 3*d* electrons to the bonding increases from VO_2 to V_2O_5 [15,16,37]. Effects stemming from this hybridization are also observed in the XES spectrum shown below.

XES is a direct probe of a materials occupied density of states. The technique becomes site specific when the energy of the incident

Table 1
Binding energy (E_B) and FWHM of the O (1*s*), V (2*p*), C (1*s*) peaks for an as grown V_2O_5 film on *c*-sapphire substrate.

Peak	Position (eV)	FWHM (eV)
O $1s_A$	530.0	1.7
O $1s_B$	530.8	3.5
V $2p_{3/2A}$	517.0	1.7
V $2p_{3/2B}$	515.5	1.5
C 1*s*	283.2	3.0

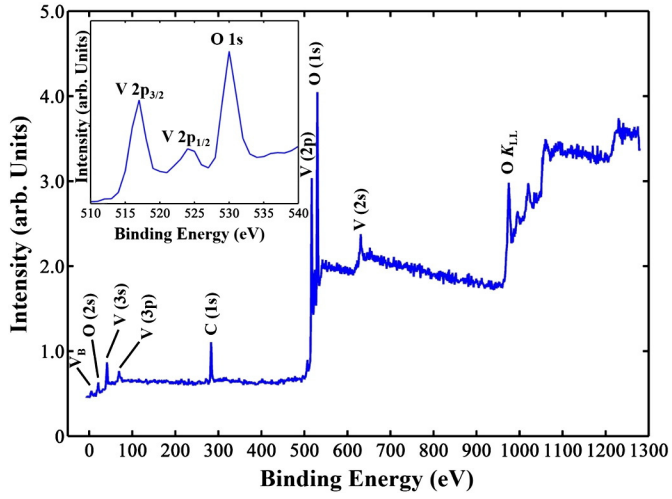

Fig. 2. Room temperature XPS spectra for V_2O_5 grown on a *c*-sapphire substrate. The inset shows V $2p_{3/2}$, V $2p_{1/2}$, and O 1*s* core level spectra.

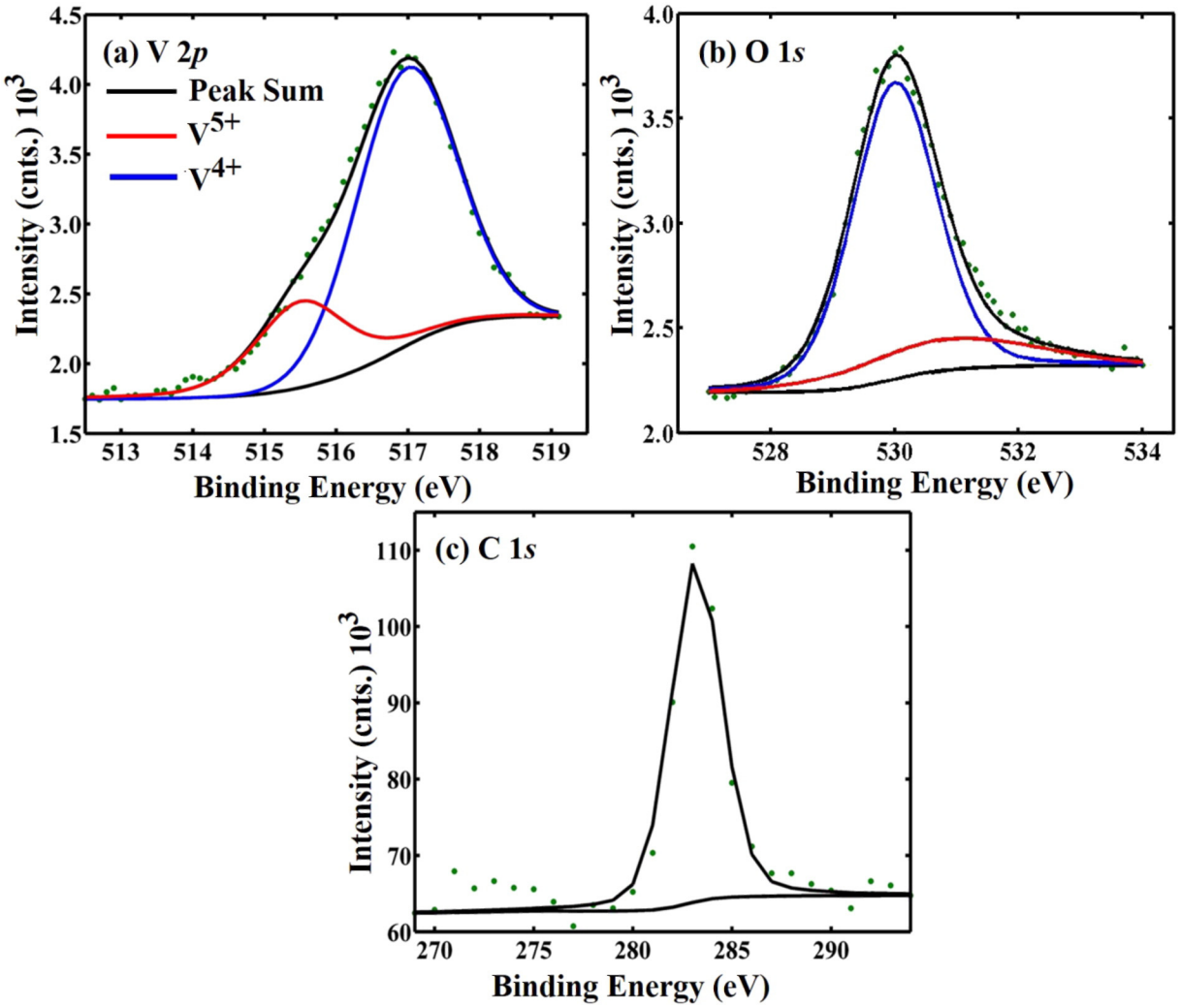

Fig. 3. V_2O_5 thin film core level XPS spectra for (a) V 2*p* and (b) O 1*s* fitted with V^{4+} and V^{5+} oxidation states and (c) C 1*s* used for calibration.

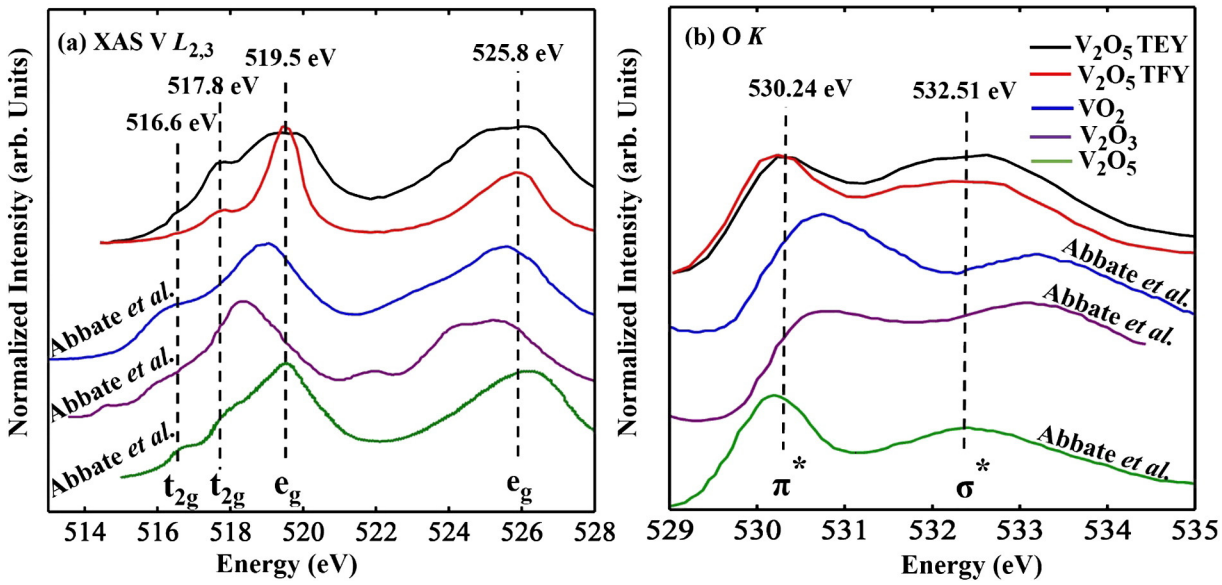

Fig. 4. XAS spectra of V_2O_5 at 300 K: (a) V $L_{3,2}$-edge, (b) O *K*-edge; where VO_2 and V_2O_3 taken from M. Abbate et al. [28] showing the dependence of splitting effects on vanadium oxidation state.

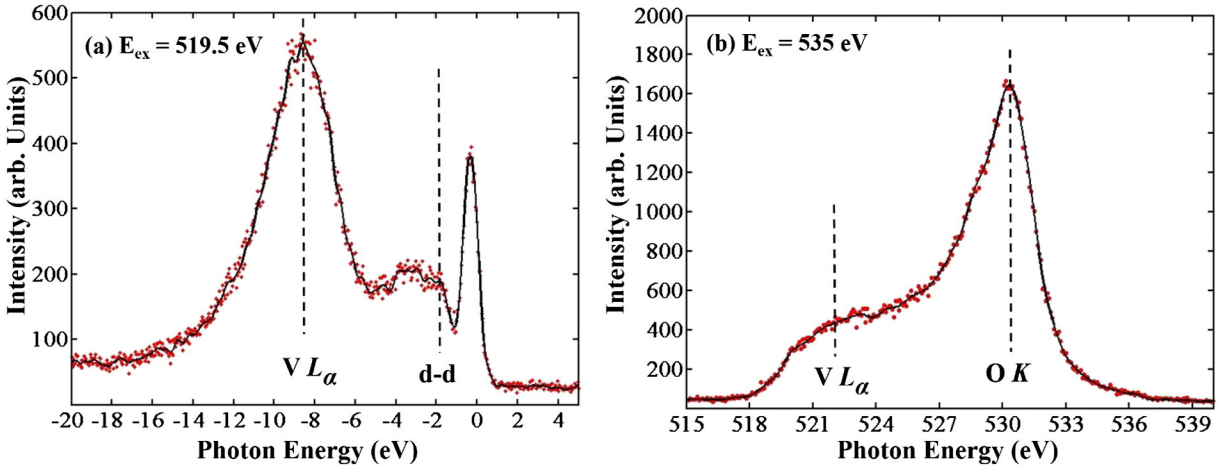

Fig. 5. XES spectra for as grown V_2O_5 samples on *c*-sapphire substrate at 300 K: (a) excited on the L_3-edge at 519.5 eV and plotted on an energy loss scale with excitation energy (b) excitation energy above the O *K*-edge at 535 eV, which shows the shift in spectral intensity from the V L_α to O *K* for different excitation energies.

radiation is tuned to that of a particular absorption feature (i.e. resonant XES, or 'RXES'). Fig. 5(a) shows the V L_α emission of the V_2O_5 thin film collected using an incident photon energy of 519.5 eV. To compare these results with those of previous studies, the V L_3-edge resonant XES spectrum was shifted to an energy loss scale relative to the elastic peak, 519.5 eV. It has been show that the broad feature at around −8.3 eV arises from the V 3d-O 2p hybridization on the L_3-edge [16]. A sub-band of local *d*-*d* transition, is found around −1.6 eV on an energy loss scale, a feature which is observed in other similar materials (Fig. 5a). While this might seem unexpected, because V^{5+} is a nominal d^0 system, there is contribution from V^{4+}, which is a d^1 system, to the −1.6 eV portion of the spectrum, due to *d*-*d* transfers within this system. The intensity of the sub-band of the local *d*–*d* excitations can be expected to be rather weak because of the small amount of V^{4+} present. These results are consistent RXES spectra at the V $L_{2,3}$ edge of V_6O_{13} oxide, performed by Schmitt et al. A prominent feature at a constant offset (~−1.6 eV) from the elastic peak was also found. The Raman-like feature was assigned in Ref. [36] to local *d*–*d* excitations within the crystal field split 3*d* multiplet (transition $e_g \rightarrow t_{2g}$). Additionally, Schmitt et al. [34] attributed features occurring at approximately −7 eV to be charge transfer transitions between V 3*d* and O 2*p* states on the V *L*-edge based on cluster model calculations [34].

Fig. 5(b) shows O *K*-edge XES for the V_2O_5 thin film. When the excitation energy is shifted from the V *L*-edge (Fig. 5a) to above the O *K*-edge threshold (Fig. 5b) there is a corresponding intensity shift from the V L_α band to the O K_α band. As expected, within Fig. 5b, the V L_β emission band (V $3d \rightarrow$ V $2p_{1/2}$) is not observed due its superposition with the more intense O K_α band [37]. It should also be noted that, due to this overlap, the V L_β band cannot be detected in VO, V_2O_3 and VO_2 [38]. To clearly observe the V L_β band for vanadium oxides, excitation for XES by an electron gun is required.

While in V_2O_5 vanadium assumes its highest formal valence charge, the V–O bonds also carry a significant covalent character, as shown in the XAS spectrum. Recent ab-initio DFT calculations of the electronic structure of V_6O_{13} indicate that vanadium contributes between 20 and 25% of the total DOS in the valence states [34].

4. Conclusions

This study described the growth and physicochemical characterization of an epitaxial V_2O_5 thin film deposited on *c*-plane sapphire. With the aid of AFM, XRD, XPS, XAS, and XES we have shown that a high quality epitaxial V_2O_5 thin film has been achieve through the simple and cheap method of thermal evaporation at relatively high pressure. AFM measurements demonstrated that the film thickness was ~50 nm with a highly smooth surface of 1.5 Å root mean square roughness. XRD measurements confirmed that the film was highly crystalline and epitaxially grown on the (0001) oriented sapphire substrate. XPS demonstrated that vanadium was predominantly in the 5+ state within the V_2O_5 thin film as determined by the shape and fitting of the core level spectra. The data suggests that increasing the partial pressure of oxygen inside a vacuum chamber would yield stoichiometric V_2O_5 films. Soft X-ray XAS and XES spectroscopy was used to probe the bulk electronic structure of the V_2O_5 thin film and verified the oxidation state of vanadium. Through this suite of techniques it was shown that relatively high pressure thermal evaporation is an efficient method of growing highly crystalline V_2O_5 thin films.

Acknowledgments

We would like to thank Dr. Wanli Yang, Jeffery Bacon, Elbara Ziade and Ruimin Qiao for their technical help and support. This research was performed in part in the Central Facilities of the Boston University, which was supported by the Boston Research Initiative. The Boston University program is supported by the Department of Energy under Grant No. DE-FG02-98ER45680. The Advanced Light Source is supported by the U.S. Department of Energy under Contract No. DE-AC02-05CH11231.

References

[1] Y. Fujita, K. Miyazaki, C. Tatsuyama, On the electrochromism of evaporated V_2O_5 films, Jpn. J. Appl. Phys. 24 (1985) 1082–1086.
[2] K. Nagase, Y. Shimizu, N. Miura, N. Yamazoe, Eletrochromic properties of spin-coated V_2O_5 thin films, Solid State Ionics 53 (1992) 490–495.
[3] P.M. Marley, G.A. Horrocks, K.E. Pelcher, S. Banerjee, Transformers: the changing phases of low-dimensional vanadium oxide bronzes, Chem. Commun. 51 (2015) 5181–5198.
[4] O.M. Osmolovskaya, I.V. Murin, V.M. Smirnov, M.G. Osmolovsky, Synthesis of vanadium dioxide thin films and nanopowders: a brief review, Rev. Adv. Mater. Sci. 36 (2014) 70–74.
[5] Y. Shimizu, K. Nagase, N. Miura, New preparation process of V_2O_5 thin film based on spin-coating from organic vanadium solution, Jpn. J. Appl. Phys. 9 (1990) L1708–L1711.
[6] D. Yu, C. Chen, S. Xie, Y. Lui, K. Park, X. Zhou, Q. Zhang, J. Li, G. Cao, Mesoporous vanadium pentoxide nanofibers with significantly enhanced Li-ion storage properties by electrospinning, Energy Environ. Sci. 4 (2011) 858–861.
[7] R. Kumar, B. Karunagaran, D. Mangalariaj, S. Narayandass, P. Manoravi, M. Joseph, V. Gopal, Pulsed laser deposited vanadium oxide thin films for uncooled infrared detectors, Sensors Actuators A 107 (2003) 62–67.
[8] S. Lee, T.L. Meyer, S. Park, T. Egami, H.N. Lee, Growth control of the oxide state in vanadium oxide thin films, Appl. Phys. Lett. 105 (2014) 223515.
[9] M.S. de Castro, C.L. Ferreira, R.R. de Avillez, Vanadium oxide thin films produced by magnetron sputtering from a V_2O_5 target at room temperature, Infrared Phys. Technol. 60 (2013) 103–107.

[10] C. Julien, J.P. Guesdon, A. Gorenstein, A. Khelfa, I. Ivanov, The influence of the substrate material on the growth of V_2O_5 flash-evaporated films, Appl. Surf. Sci. 90 (1995) 389–391.
[11] L. Murawski, C. Gledel, C. Sanchez, J. Livage, J.P. Audieres, Electrical conductivity of V_2O_5 and $Li_xV_2O_5$ amorphous thin films, J. Non-Cryst. Solids 89 (1987) 98–106.
[12] C.V. Ramana, O.M. Hussain, B. Srinivasulu Naidu, P.J. Reddy, Spectroscopic characterization of electron-beam evaporated V_2O_5 thin films, Thin Solid Films 305 (1997) 219–226.
[13] G. Silversmit, D. Depla, H. Poelman, G.B. Marin, R.D. Gryse, Determination of the V2p XPS binding energies of different vanadium oxidation states (V^{5+} to V^{0+}), J. Electron Spectrosc. Relat. Phenom. 135 (2004) 167–175.
[14] X.J. Wang, H.D. Li, Y.J. Fei, X. Wang, Y.Y. Xiong, Y.X. Xiong, Y.X. Nie, K.A. Feng, XRD and Raman study of vanadium oxide thin films deposited on fused silica substrates by RF magnetron sputtering, Appl. Surf. Sci. 177 (2001) 8–14.
[15] S. Guimond, J.M. Sturm, D. Gobke, Y. Romanyshyn, M. Naschitzki, H. Kuhlenbeck, H.-J. Freund, Well-ordered V_2O_5 (001) thin films on Au (111) growth and thermal stability, J. Phys. Chem. C 112 (2008) 11835–11846.
[16] J. Laverock, A.R.H. Preston, B. Chen, J. McNulty, K.E. Smith, L.F.J. Piper, P.A. Glans, J.H. Guo, C. Marin, E. Janod, V. Ta Phoc, Orbital anisotropy and low-energy excitations of the quasi-one-dimensional conductor β-$Sr_{0.17}V_2O_5$, Phys. Rev. B 84 (2011) 155103.
[17] J. Laverock, A.R.H. Preston, D. Newby Jr., K.E. Smith, S. Sallis, L.F.J. Piper, S. Kittiwatanakul, J.W. Lu, S.A. Wolf, M. Leandersson, T. Balasubramanian, Photoemission evidence of crossover from Peierls-like to Mott-like transition in highly strained VO_2, Phys. Rev. B 86 (2012) 195124.
[18] R. Lindstrom, V. Maurice, S. Zanna, L. Klein, H. Groult, L. Perrigaud, C. Cohen, P. Marcus, Thin films of vanadium oxide grown on vanadium metal: oxidation conditionsto produce V_2O_5 films of Li-intercalation applications and characterization of XPS, AFM, RBS/NRA, Surf. Interface Anal. 38 (2006) 6–18.
[19] B. Jovic, Synchronization Techniques for Chaotic Communication Systems, first ed., 2011 (Hamburg, Germany).
[20] E.C. Ifeachor, B.W. Jervis, Digital Signal and Processing: A Practical Approach, fifth ed., 2002 (Wokingham, UK).
[21] V. Brázdová, V. Ganduglia-Pirovano, M. Sauer, Periodic density functional study on structural and vibrational properties of vanadium oxide aggregates, Phys. Rev. B 69 (2004) 165420.
[22] T. Blanquart, J. Niinisto, M. Gavagnin, V. Longo, M. Heikkila, E. Puukilainen, V. Pallem, C. Dussarrat, M. Ritala, M. Leskela, Atomic layer deposition and characterization of vanadium oxide thin films, RSC Adv. 3 (2013) 1179–1185.
[23] J.S. Mrowiecka, F. Martin, V. Maurice, S. Zanna, L. Klein, J. Castle, P. Marcus, The distribution of lithium intercalated in V2O5 thin films studied by XPS and ToF-SIMS, Electrochim. Electrochim. Acta 53 (2008) 4257–4266.
[24] A. Benayad, H. Martinem, A. Gies, B. Pecquenard, A. Lavasseur, D. Gonbeau, Effect of total gas and oxygen partial pressure during deposition on properties of sputtered V_2O_5 thin films, J. Electron Spectrosc. 150 (2006) 1627–1634.
[25] J. Mendialdua, R. Casanova, Y. Barbaux, XPS studies of V_2O_5, V_6O_{13}, VO_2, V_2O_3, J. Electron Spectrosc. Relat. Phenom. 71 (1995) 249–261.
[26] B.M. Reddy, I. Ganesh, E. Reddy, A. Gernandez, P. Smirniotis, Surface characterization of Ga_2O_3-TiO_2 and V_2O_5/Ga_2O_3 catalysts, J. Phys. Chem. 105 (2001) 6227–6235.
[27] G. Beamson, D. Briggs, High Resolution XPS of Organic Polymers, the Scienta ESCA 300 Database, John Wiley & Sons, 1992.
[28] N. Ibris, A.M. Salvi, M. Liberatore, F. Decker, A. Surca, XPS study of the Li intercalation process in sol-gel produced V_2O_5 thin film: influence of substrate and film synthesis modification, Surf. Interface Anal. 37 (2005) 1092–1104.
[29] A.M. Salvi, M.R. Guascito, A. DeBonis, F. Simone, A. Pennisi, F. Decker, Lithium intercalation on amorphous V_2O_5 thin film, obtained by rf deposition, using in situ sample transfer for XPS analysis, Surf. Interface Anal. 35 (2003) 897–905.
[30] S. Shin, S. Suga, M. Taniguchi, M. Fujisawa, H. Kanzaki, A. Fujimori, H. Daimon, Y. Ueda, K. Kosuge, S. Kachi, Vacuum-ultraviolet reflectance and photoemission study of the metal-insulator phase transition in VO_2, V_6O_{13}, and V_2O_3, Phys. Rev. B 41 (1990) 4993.
[31] J. Zaanen, G.A. Sawatzky, J. Fink, W. Speier, J.C. Fuggle, $L_{2,3}$ adsorption spectra of the lighter 3d transition metals, Phys. Rev. B 32 (1985) 4905.
[32] D.W. Fischer, Molecular-orbital interpretation of the soft X-ray $L_{II,III}$ emission and absorption spectra from some titanium and vanadium compounds, J. Appl. Phys. 41 (1970).
[33] D.W. Fischer, Soft X-ray band spectra and molecular orbital structure of Cr_2O_3, CrO_3, CrO_4^{-2} and $Cr_2O_7^{-2}$, J. Phys. Chem. Solids 32 (1971) 2455–2480.
[34] T. Schmitt, L.-C. Duda, M. Matsubara, M. Mattesini, M. Klemm, A. Augustsson, J.-H. Guo, T. Uozumi, S. Horn, R. Ahuja, A. Kotani, J. Nordgren, Electronic structure studies of V_6O_{13} by soft X-ray emission spectroscopy: band-like and excitonic vanadium states, Phys. Rev. B 69 (2004) 125103.
[35] M. Abbate, The O 1s and V 2p X-ray absorption spectra of vanadium oxides, Braz. J. Phys. 24 (1994) 785–795.
[36] M. Abbate, H. Pen, M.T. Czyiyk, F.M.F. de Groat, J.-C. Fuggleav, Y.J. Ma, C.T. Chen, F. Sette, A. Fujimori, Y. Ueda, K. Kosuge, Soft X-ray absorption spectroscopy of vanadium oxides, J. Electron Spectrosc. Relat. Phenom. 62 (1993) 185–192.
[37] Y. Ishiwata, S. Suehiro, Y. Soi, Y. Tezuka, O. Morimoto, X.-G. Zheng, Metal-insulator transition for V_2O_3 powder observed using a soft X-ray emission spectrometer, J. Phys. Soc. Jpn. 79 (2010) 05472.
[38] O.Y. Khyzhun, T. Struskus, W. Grunert, C. Woll, Valence band electronic structure of V_2O_5 as determined by resonant soft X-ray emission spectroscopy, J. Electron Spectrosc. Relat. Phenom. 149 (2005) 45–50.